Membrane Water Treatment, Vol. 4, No. 1 (2013) 53-67
DOI: http://dx.doi.org/10.12989/mwt.2013.4.1.053

Study of the ageing of hollow fibers in an industrial module for drinking water production

S. Wang[1,3a], Y. Wyart[*1], J. Perot[2], F. Nauleau[2] and P. Moulin[1]

[1]*Aix Marseille Université, Laboratoire de Mécanique, Modélisation et Procédés Propres (M2P2 – UMR-CNRS 7340), Europôle de l'Arbois, BP. 80, Bâtiment Laennec, Hall C, 13545 Aix en Provence Cedex 04, France*
[2]*SAUR, 1 avenue Eugène Freyssinet, 78064 Saint Quentin en Yvelines Cedex, France*
[3]*School of Environmental Science and Engineering, Huazhong University of Science and Technology, 430074 Wuhan, China*

(Received July 19, 2012, Revised January 15, 2013, Accepted January 22, 2013)

Abstract. In this study, ageing characteristics of an industrial hollow-fiber membrane module were investigated after 50 months of drinking water production. For this purpose, the industrial module was opened to make 18 smaller modules with hollow-fibers taken from different parts of the industrial module. These modules were probed by the use of a magnetic nanoparticle (NP) challenge test based on magnetic susceptibility (K) measurement of permeate. No magnetic susceptibility was detected in permeate when the challenge test was performed on an intact membrane module, indicating the complete retention of nanoparticles by the membrane. The compromised membrane module can be successfully detected by means of magnetic susceptibility measurement in permeate. So, this study clearly demonstrates that ageing of ultrafiltration membranes can be monitored by measuring the magnetic susceptibility of permeate from an ultrafiltration membrane module. These results showed that the hollow fibers in the center zones of the bundle would age faster than those in the outer zones around the bundle. This result is in agreement with numerical simulation (Daurelle *et al*. 2011).

Keywords: drinking water, ageing characteristics, magnetic nanoparticles, magnetic susceptibility

1. Introduction

The ultrafiltration membrane is increasingly being used in drinking water treatment because of its complete removal of pathogens, such as Giardia, Cryptosporidium and viruses. Membrane ageing or loss of membrane integrity causes a drop in removal efficiency and threatens downstream use. Therefore in order to maintain reliability, it is common practice to regularly check membrane integrity to confirm reliable filtration performance during the operation.

A wide range of physical and biological techniques, such as particle counting, particle monitoring, turbidity monitoring, sonic sensor tests, air pressure tests, bubble pressure tests, bacteriophage challenge tests and routine microbial analysis have been applied to membrane

*Corresponding author, Associate Professor., E-mail: yvan.wyart@univ-amu.fr
[a] Ph.D., E-mail : wangsonglin99@126.com

integrity monitoring (Guo *et al.* 2010a). All of these techniques are aimed at distinguishing changes in physical, chemical and/or biological conditions between intact and compromised membranes. Of these, the pressure decay test and the diffusive air flow test are the most frequently used direct methods and they are considered to be simple, non-destructive and reliable methods. Conventional indirect methods are applied to measure water quality in the permeate solution, i.e., particle counting, particle monitoring, turbidity monitoring and different surrogate challenge tests (Walsh *et al.* 2005). Other different membrane integrity methods (Laîné *et al.* 1998, Giglia *et al.* 2008, DiLeo *et al.* 1995, Phattaranawik *et al.* 2008, Choi *et al.* 2011) (e.g., acoustic sensor method, liquid-liquid porosimetry, binary gas integrity test, new membrane-based sensor and fluorescent silica particles) are also able to detect any loss in membrane integrity. The novel membrane integrity test, proposed by Moulin (2008), can be classified as a direct method and uses Fe_3O_4 magnetic nanoparticles (NP) as a surrogate detector of membrane damage. If a membrane is damaged, the magnetic nanoparticles are discovered in permeate. Guo *et al.* (2010b) investigated the minimum detection level of this alternative ultrafiltration membrane integrity test based on magnetic nanoparticles and measurement of magnetic susceptibility (K). This surrogate challenge test for ultrafiltration membrane integrity monitoring is revealed as a plausible solution for large-scale applications with the advantages of simplicity, on-line operation, accurate and quick detection, high specificity, high sensitivity and very low influence on membrane fouling.

Cracking of membrane fibers can result from chemical attack such as oxidation or chemical cleaning, faulty installation and maintenance, high fouling, membrane stress and strain from operating conditions and damage by sharp objects not removed by pretreatment (Suh *et al.* 2011). Recently, attention has been directed towards membrane life estimation, the effect of cleaning agents on membrane ageing and the effect of ageing on membrane performance. So far, no study has appropriately investigated the difference of ageing characteristics along different parts of membrane modules. The cracking of membrane fibers cannot be predicted through their position and/or operating conditions.

The main objective of this paper is to use magnetic nanoparticles in order to study the difference in ageing characteristics along different parts of industrial hollow-fiber membrane modules.

2. Materials and methods

2.1 Preparation of magnetic nanoparticles

Fe_3O_4 magnetic nanoparticles were prepared by the chemical co-precipitation of ferrite (Fe^{3+}) and ferrous (Fe^{2+}) salts with the molar ratio of 2:1 using ammonium hydroxide (NH_4OH) as the precipitating agent. The chemical reaction is:

$$2Fe^{3+} + Fe^{2+} + 8OH^- \rightleftharpoons Fe(OH)_2 + 2\,Fe(OH)_3 \rightarrow Fe_3O_4 + H_2O$$

To avoid particle aggregation or adhesion, the synthesized Fe_3O_4 nanoparticles were stabilized with meso-2, 3-dimercapto-succinic acid (DMSA) (Fauconnier *et al.* 1997, Guo *et al.* 2010b). After the magnetic nanoparticle solution was acidified slowly with 0.05 M HCl to pH = 2, the DMSA was added and stirred for 30 minutes. The ratio of added DMSA to [Fe] is 3.5%. Then the pH value of the solution was adjusted from 2 to 11, and from 11 to 7 by slowly adding 0.05 M NaOH and 0.05 M HCl, respectively.

2.2 Characterization of magnetic nanoparticles

The prepared Fe_3O_4 nanoparticles were characterized in terms of size distribution and magnetic susceptibility. The nanoparticle size distribution was determined by a Malvern Zetasizer granulometer (ZEN 1600, Malvern Instrument, UK), based on dynamic light scattering measurement. The magnetic susceptibility of Fe_3O_4 nanoparticles was measured by means of a Bartington magnetic susceptibility meter equipped with a MS2B sensor (Bartington Instrument, UK) and an AGICO Kappabridge magnetic susceptibility meter (MFK1-FA, AGICO Instrument, Czech Republic). Bartington instruments can display values from 0.1 to 9999 (e.g., (0.1~9999)* 10^{-5} SI for volume magnetic susceptibility), providing a very wide analytical range for detecting magnetic material. Generally, the response time for measuring a sample is 2 or 12 seconds depending on the selected measurement range. In contrast, the AGICO Kappabridge magnetic susceptibility meter has the same advantages of a very wide analytical range as well as rapid detection. Moreover, it offers more detection sensitivity (the minimum detection limit is $0.2*10^{-6}$ SI). The nanoparticle magnetic susceptibility was obtained by subtracting magnetic susceptibility of water from that of samples.

2.3 Ultrafiltration membrane module and integrity tests

An industrial membrane module of 10,000 polyethersulfone fibers (area = 35 m²), whose nominal molecular weight cut-off is 150 kDa, has been used for 50 months in a SAUR pilot plant. The mean pore size of this membrane is about 25 nm. The industrial module was divided into the following parts (Fig. 1) by Polymem society to study 4 effects:

- Distribution of the fibers in the module (1, 2, 3 and 4),
- Length of the module: 1st third (5 and 8), 2nd third (6 and 9), 3rd third (7 and 10),
- Periphery / center of a bundle (A, B and C, D),
- Upper / lower parts of a bundle (E, F and G, H).

For each module, hollow fibers are used to create modules as representative as possible. For example, for module 1; 700 hollow fibers are taken randomly from the bundle, for module D; 400 hollow fibers are taken randomly from amongst fibers in the center of the bundle. The modules N1 and N2 are made from hollow fibers taken from a new industrial unit. These serve as a reference to this study. The characteristics of the different modules are given in Table 1.

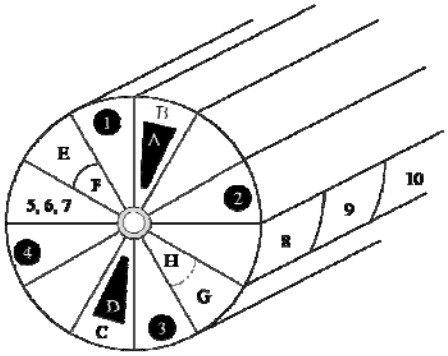

Fig. 1 The different investigated parts of the industrial module

Table 1 Tested module characteristics

	1, 2, 3, 4	A, B, C, D / E, F, G, H	5, 6, 7 / 8, 9, 10
Number of hollow fibers	700	400	300
Membrane area (m²)	1.26	0.73	0.21
Module diameter (mm)	90	70	60
Module length (mm)	800	800	300

2.4 Experimental plant

The ultrafiltration plant is described in Fig. 2. It consists of a 100 L (BO 1) tank of concentrate and 50 L (BO 2) tank of permeate. The centrifugal pump (PO 1) supplies the membrane module from the concentrate tank (flow rate: 5 m^3 h^{-1}). The permeate can be used to backwash the membrane module using a pump (PO 2) providing a flow of 500 L h^{-1}. The rates of these two pumps are controlled and are measured by flow-meters (FLO 1 and FLO 3). Pressure gauges (Pi 1, Pi 2, and Pi 3) are used to measure the pressure on the two fluids and a valve at the exit of the membrane (NVO 1) is used to determine the TMP (trans-membrane pressure).

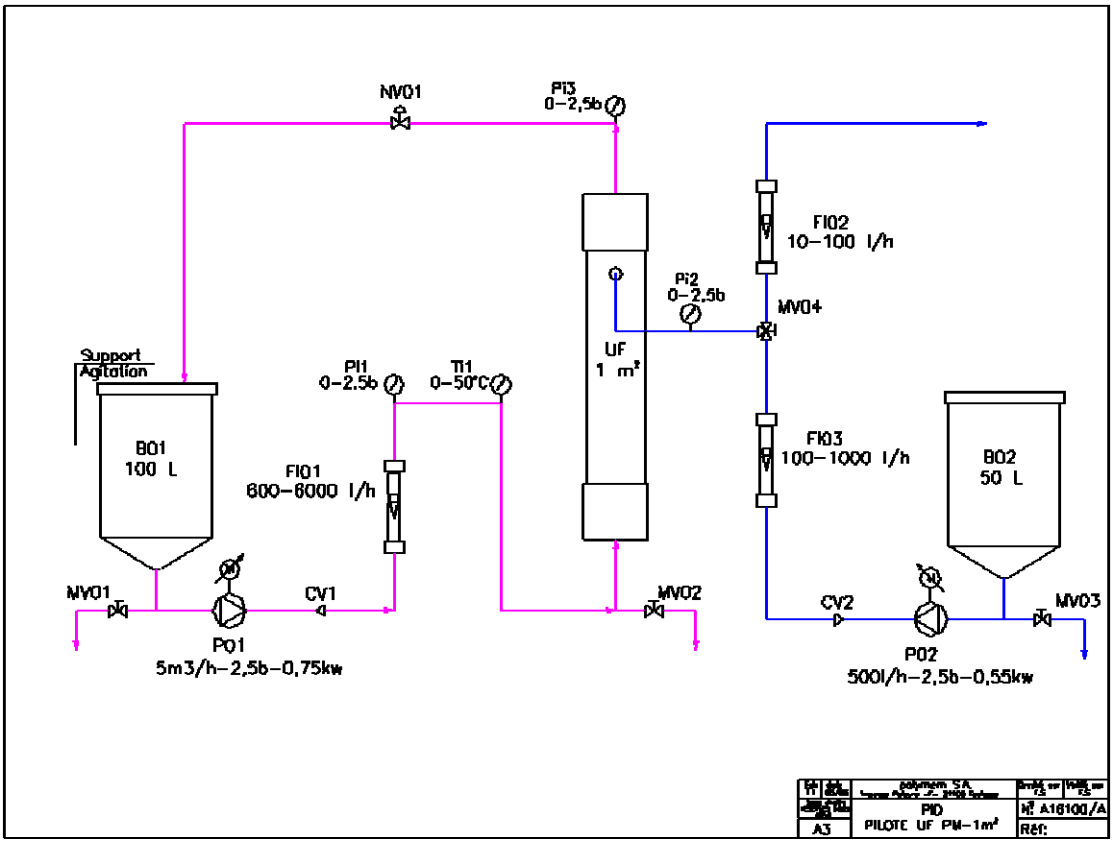

Fig. 2 Experimental plant

This plant is equipped with the modules described in Table 1. The tests were performed at constant volume (permeate and retentate returned in the feed tank).

All the membrane modules were backwashed with distilled water for 20 minutes and were then characterized by water permeability measurement prior to magnetic NP test.

After obtaining a satisfactory initial permeability, the pilot is filled with 15 L of distilled water (with 5 L of dead volume). An experiment consists of three additions of 100mL of nanoparticle suspensions (t0, t0+10' and t0+20') and for each addition there are 3 samples of feed and permeate (t0+2', t0+5' and t0+10'). To summarize, 18 samples are taken (t0+2', t0+5', t0+10', t0+12', t0+15', t0+20', t0+22', t0+25' and t0+30') for the permeate and feed. All the experiments were performed to constant permeate flow (120 $L.h^{-1}$ recycled in the feed) and TMP (0.2 bar). The magnetic susceptibility of permeate was measured to investigate whether nanoparticles had passed through the membrane or not. After each test, the membrane module was rinsed well with distilled water and was then back-washed using distilled water at 2 bar to assess the membrane regeneration performances.

In parallel, the integrity of each module was tested using the air bubble test method to check if the results are in agreement or not. The test pressure and the duration were 1 bar and 5 minutes, respectively.

3. Results and discussion

3.1 Fiber characterization

A surface heterogeneity of the hollow fibers was observed with 50% being of a yellowish color and 50% being covered with PAC (Powdered Activated Carbon, black color). Complementary EDX analysis shows the presence of Fe (coagulant used in pretreatment), sulfur (issued from the material) and to a lesser degree silica, aluminum and chlorine. It was therefore later decided to perform a backwash of all modules at 1.5 bar in pretreatment to remove the maximum PAC and achieve maximum permeability of the used modules. This value of permeability is between 400 and 650 $L.h^{-1}.m^{-2}.bar^{-1}$. However, in comparison with new modules during experiments with nanoparticles there appears to be an adsorption of the latter. Initial tests on used modules 1, 2, 3 and 4 showed the presence of PAC in hollow fibers despite the preventive backwash. Indeed, monitoring the magnetic susceptibility over time for these modules revealed a significant drop which can be explained by the adsorption of magnetic nanoparticles on PAC.

3.2 Characterization of new membranes (N1 and N2)

Table 2 summarizes all the parameters of experiments on modules N1 and N2. The permeability of the modules was about 700 $L.h^{-1}.m^{-2}.bar^{-1}$. In Table 2, the average diameter of nanoparticles present in the feed can also be found. This data, on the whole experiment, is obtained by averaging the nine values obtained for each sample (t0+2', t0+5', t0+10', t0+12', t0+15', t0+20', t0+22', t0+25' and t0+30'). It can be noted that nanoparticles of initial suspensions have a size of 50-70 nm. This size increases slightly after 30 minutes of experiment.

The magnetic susceptibility K of the N2 module remains acceptable (3553.10^{-6} SI) even if a little weak. The evolution of the magnetic susceptibility K in the feed and permeate is shown on Fig. 3.

Table 2 Parameters for the experiments with the modules N1 and N2

Module	Lp0 at 20°C ($L.h^{-1}.m^{-2}.bar^{-1}$)	NP MD (nm) Initial suspension	K (10^6 SI) Initial suspension	NP MD (nm) Feed
N1	630	52	5073	68
N2	730	73	3553	101

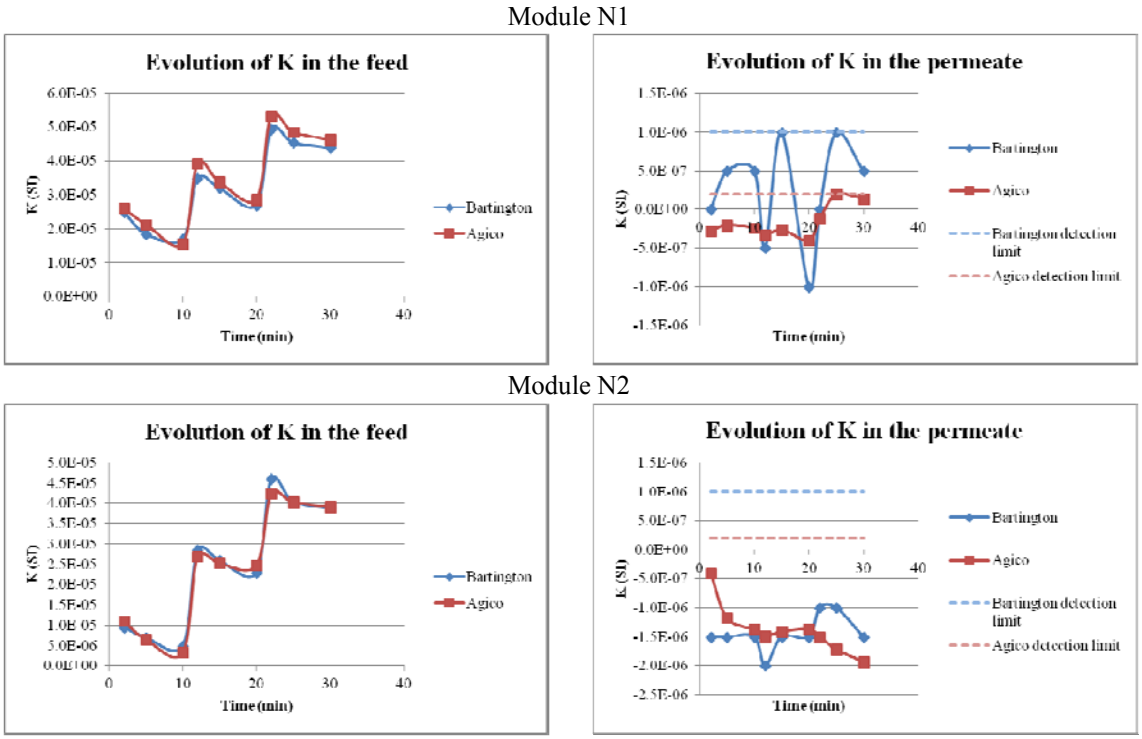

Fig. 3 Variation of the magnetic susceptibility in the feed (left) and in the permeate (right) as a function of time [modules N1 and N2]

The curves show clearly that the 2 modules are intact, an expected result confirmed by the air test. The module backwash can easily recover the initial permeability of the membranes. All of these results confirm once more the work of Guo *et al*. (2010b).

3.3 Characterization of the used membranes

3.3.1 Effect of the position in the bundle

Table 3 summarizes all the parameters of experiments on modules 1, 2, 3 and 4. After backwashing, the permeability of the modules, between 436 and 550 $L.h^{-1}.m^{-2}.bar^{-1}$, can be considered equivalent. It can be noted that the initial suspensions are not exactly homogeneous with a greater size of nanoparticles for module 1 (67 nm) and a weaker magnetic susceptibility K for module 2 (3506.10^{-6} SI). However, these values are perfectly satisfying for the ageing test. The average diameter of the nanoparticles in the feed shows that the 30 minutes of experiment have a low influence on the geometric properties of the nanoparticles. The evolution of the magnetic

Table 3 Parameters for the experiments with the modules 1, 2, 3 and 4

Module	Lp0 at 20°C ($L.h^{-1}.m^{-2}.bar^{-1}$)	NP MD (nm) Initial suspension	K (10^6 SI) Initial suspension	NP MD (nm) Feed
1	532	67	8486	112
2	496	53	3506	51
3	550	51	7945	72
4	436	54	5203	62

susceptibility K in the feed and the permeate is shown in Fig. 4. It can be observed that even if the modules have been backwashed, there must be some PAC leftover in the hollow fibers because if each addition of nanoparticles increases the feed concentration, this latter is followed by a decrease until the following addition. In comparison, this drop is more important than for the new modules N1 and N2 which don't contain PAC: in that case, there is no nanoparticles adsorption on new membranes (Guo 2009) and only the homogenization of the feed explains this drop. The analysis of the evolution of the magnetic susceptibility in the permeate clearly shows that modules 2, 3 and 4 are intact (confirmation by air test). However, if the Bartington apparatus doesn't allow us to detect a defect in module 1, the Agico apparatus clearly shows the ageing and the loss of integrity of this module. The default associated to this loss of integrity must be relatively low as the air test fails to highlight the ageing of the module. The module backwash allows us to easily recover the initial permeability of the membranes.

3.3.2 Effect of the length of the module (5, 8), (6, 9) and (7, 10)

Table 4 summarizes all the parameters of experiments done on modules (5, 8), (6, 9) and (7, 10). After backwashing, the modules permeability was around 500 $L.h^{-1}.m^{-2}.bar^{-1}$, apart from module 7 which had permeability comparable to that of the new hollow fibers (642 $L.h^{-1}.m^{-2}.bar^{-1}$).

However, this does not happen with the permeability of module 10 (identical to module 7 but placed at 180° from the latter) which nevertheless has a high permeability. The initial suspensions are homogeneous apart from the magnetic susceptibility K of module 5 (3506.10^{-6} SI). The average diameter of the nanoparticles in the feed shows that 30 minutes of experiment had no effect on the properties of the nanoparticles of modules 5, 7, 8 et 9. For modules 6 and 10, a slight increase in the average diameter of the nanoparticles is observed. The evolution of the magnetic susceptibility K in the feed and the permeate is shown in Fig. 5. As in the case of modules 1, 2, 3 and 4, residual PAC must be present in the hollow fibers as each addition of nanoparticles is followed by a strong decrease in concentration until the next addition. The analysis of the evolution of the magnetic susceptibility in the permeate clearly shows that modules 5, 7, 8, 9 and 10 are intact (confirmed by air test).

The same conclusion can be drawn regarding module 6: even if 2 points are above the detection limit in the case of the Bartington equipment, this cannot be considered categorically as a lack of integrity (Guo *et al.* 2010b). The air test did not reveal any abnormality on module 6. The backwash of the module allowed us to easily recover the initial permeability of the membranes.

3.3.3 Effect of periphery (B, C) / centre (A, D) of the bundle

Table 5 summarizes all the parameters of experiments on modules (A, D) and (B, C). After backwashing, the permeability of the modules was homogeneous, around 500 $L.h^{-1}.m^{-2}.bar^{-1}$. Among the initial suspensions, one has rather large nanoparticles (B, 105 nm) and one has

Module 1

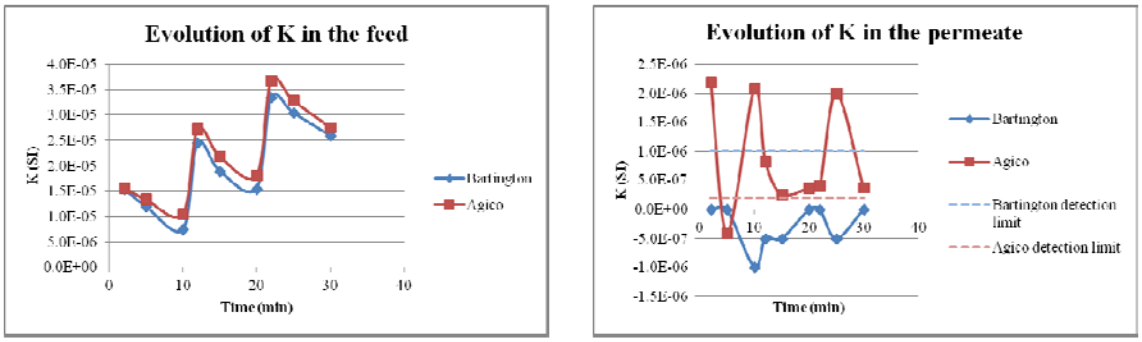

Module 2

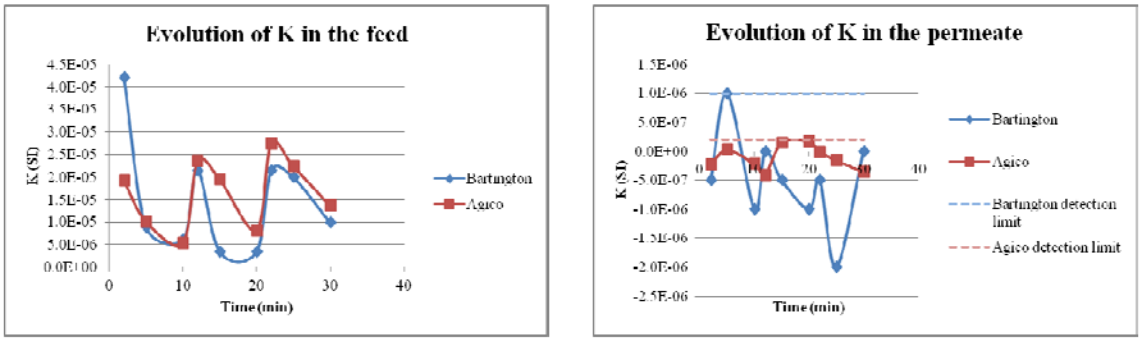

Module 3

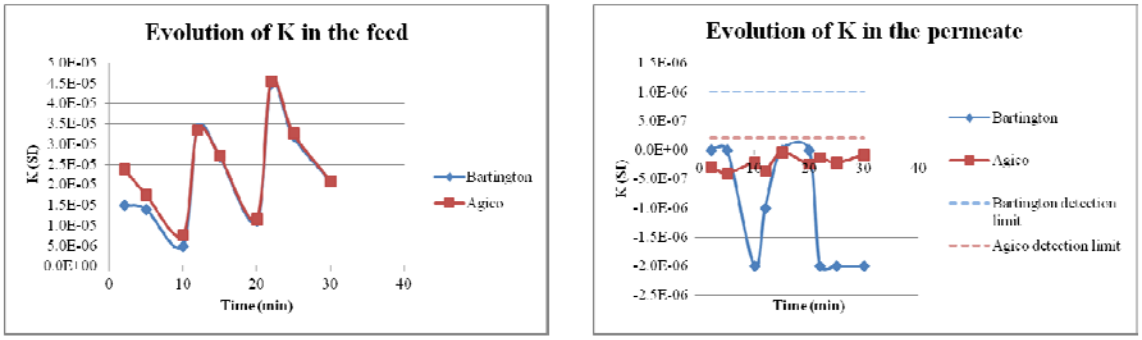

Module 4

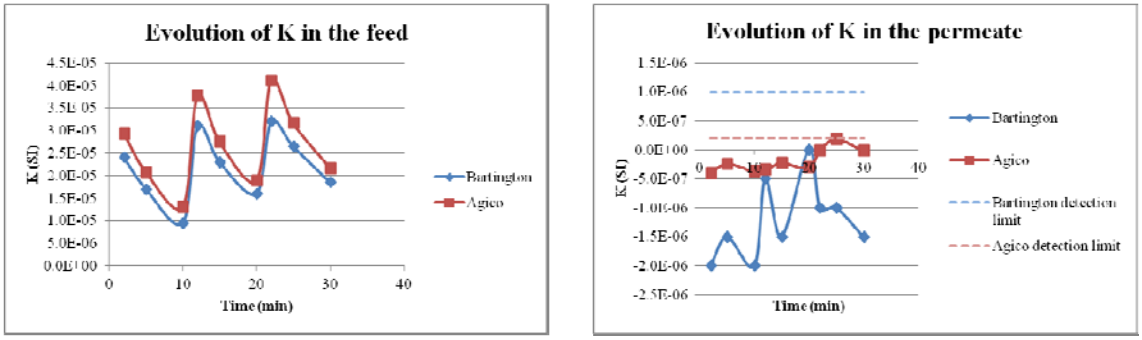

Fig. 4 Variation of the magnetic susceptibility in the feed (left) and in the permeate (right) as a function of time [modules 1, 2, 3 and 4]

Table 4 Parameters for the experiments with the modules (5, 8), (6, 9) and (7, 10)

Module	Lp0 at 20°C ($L.h^{-1}.m^{-2}.bar^{-1}$)	NP MD (nm) Initial suspension	K (10^6 SI) Initial suspension	NP MD (nm) Feed
5	507	53	3506	51
8	461	65	5723	70
6	478	70	4743	100
9	507	65	5398	60
7	642	54	4876	57
10	509	70	4749	105

Module 5

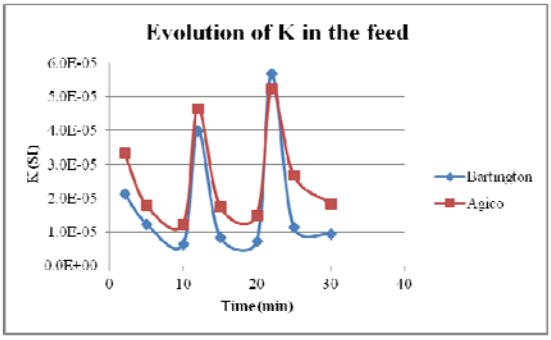

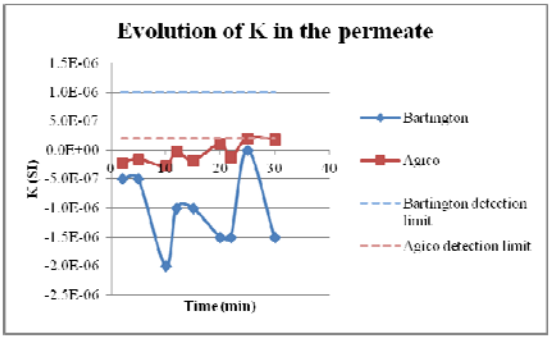

Module 8

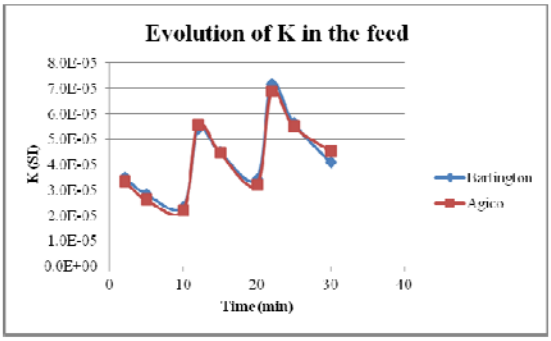

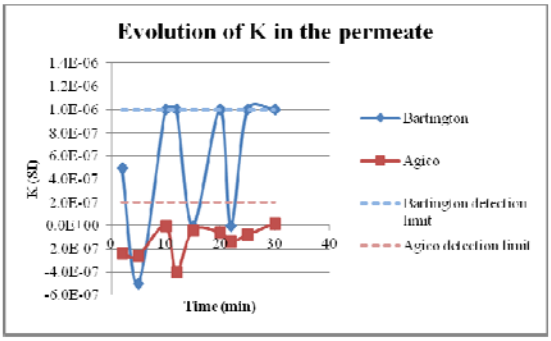

Module 6

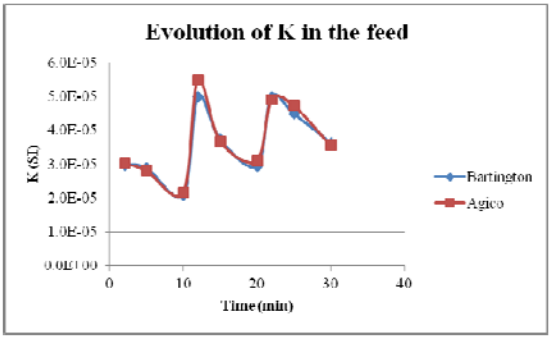

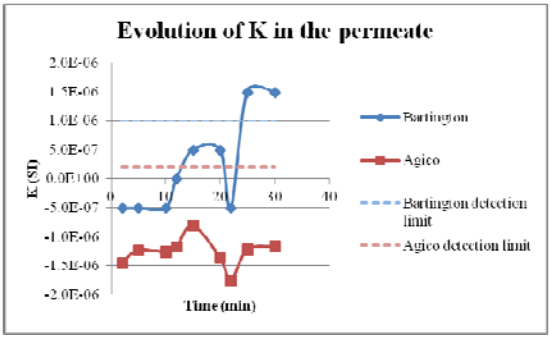

Fig. 5 Continued

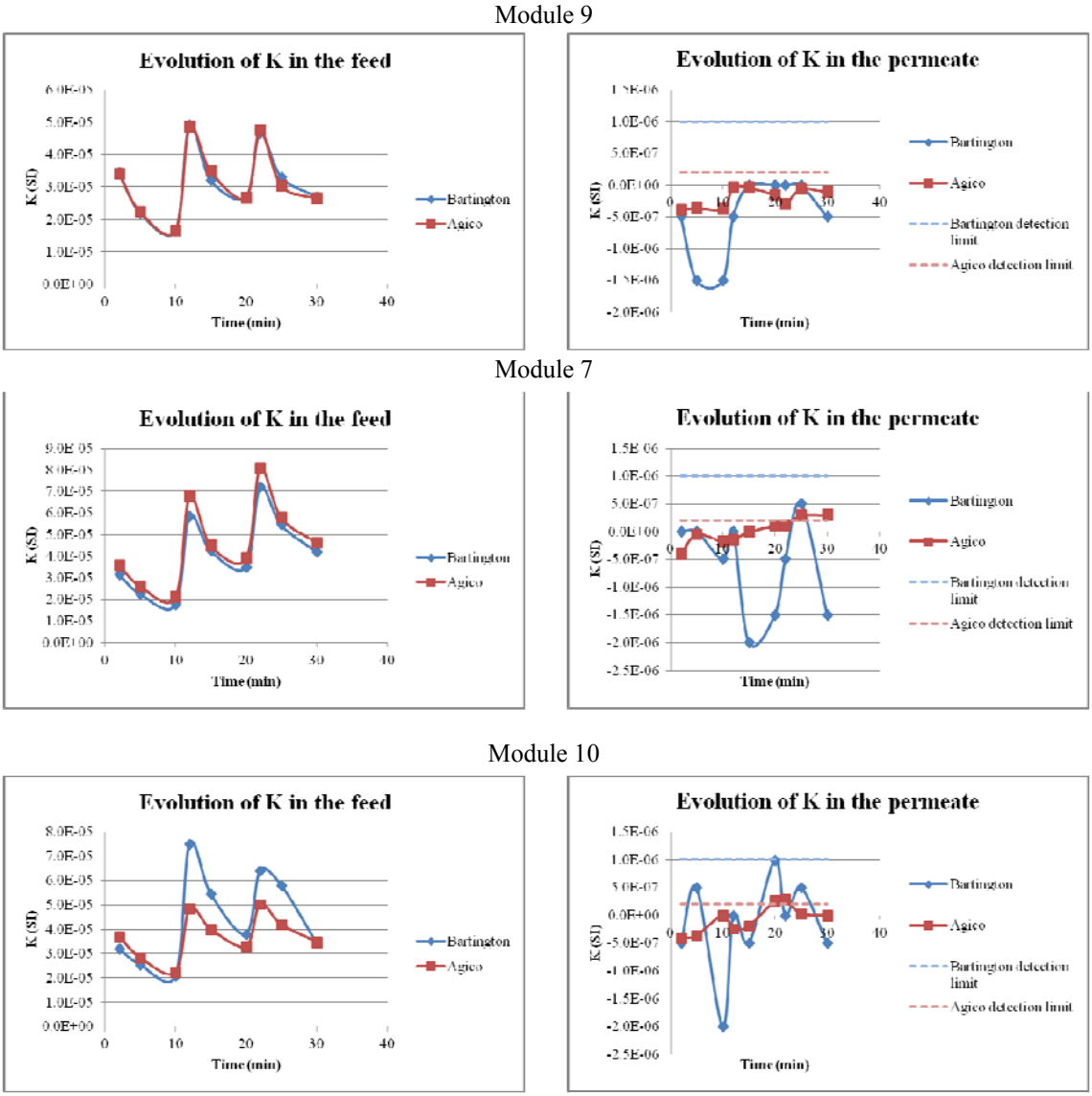

Fig. 5 Variation of the magnetic susceptibility in the feed (left) and in the permeate (right) as a function of time [modules 5 and 8 (first third of the module length) ; 6 and 9 (secon d third of the module length); 7 and 10 (third third of the module length)]

relatively small nanoparticles (A, 23 nm). No suspension was strongly influenced during the experiment. The evolution of the magnetic susceptibility K in the feed and the permeate is shown in Fig. 6. As for the previously used modules, the same observation and the same conclusion can be made regarding the evolution of the magnetic susceptibility in the feed (presence of PAC). The analysis of the evolution of the permeability in the permeate clearly shows that modules B and C, corresponding to the fibers at the periphery of the bundle, are intact (confirmed by air test).

However, the measurement of the magnetic susceptibility shows that modules A and D (located at 180° of module A), corresponding to fibers at the center of the bundle, present an advanced ageing with a lack of integrity. For module A, this initial conclusion could have originated from a nanoparticle size too small (about the size of the pores of the membrane), but the air test has clearly demonstrated the presence of defects. The air test was also positive in the case of module D. This result can be correlated with the results in numerical simulation (Daurelle *et al.* 2011). In a bundle, it was shown that during the backwash the pressure applied to the hollow fibers could fall by 10-15% between the hollow fibers at the periphery and the hollow fibers at the centre of the bundle, whilst this percentage varied very little during the filtration (0.4%). This results in a lower efficiency of backwashing for hollow fibers at the center, a residual clogging increasing over time and an accelerated ageing at this point of the bundle. As with other modules, the backwashing of the module allowed us to easily recover the initial permeability of the membranes.

3.3.4 Effect of lower parts (F, H) / upper parts (E, G) of the bundle

Table 6 summarizes all the parameters of experiments on modules (F, H) and (E, G). After backwashing, the permeability of the modules is homogeneous, around 500 $L.h^{-1}.m^{-2}.bar^{-1}$. Among the initial suspensions, suspension H has very little nanoparticles (18 nm) even if this size is doubled during the experiment (36 nm). The other suspensions are not strongly influenced during the experiment. The evolution of the magnetic susceptibility K in the feed and permeate is shown in Fig. 7. As for the previously used modules, the same observations and the same conclusions can be made regarding the evolution of the magnetic susceptibility in the feed (presence of PAC).

The analysis of the evolution of the permeability in the permeate clearly shows that modules F and G, are intact (confirmed by air test). However, the measurement of the magnetic susceptibility

Table 5 Parameters for the experiments with the modules (A, D) and (B, C)

Module	Lp0 at 20°C ($L.h^{-1}.m^{-2}.bar^{-1}$)	NP MD (nm) Initial suspension	K (10^6 SI) Initial suspension	NP MD (nm) Feed
A	516	23	4954	26
D	531	41	7041	50
B	520	105	3350	110
C	504	67	6559	100

Module A

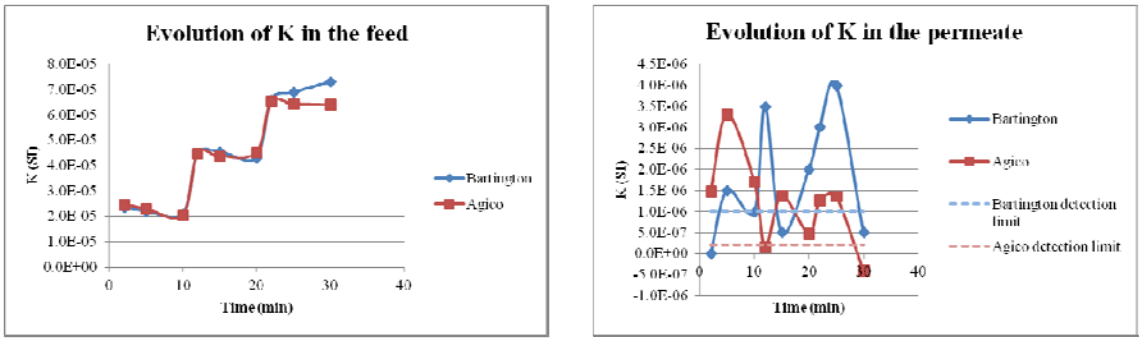

Fig. 6 Continued

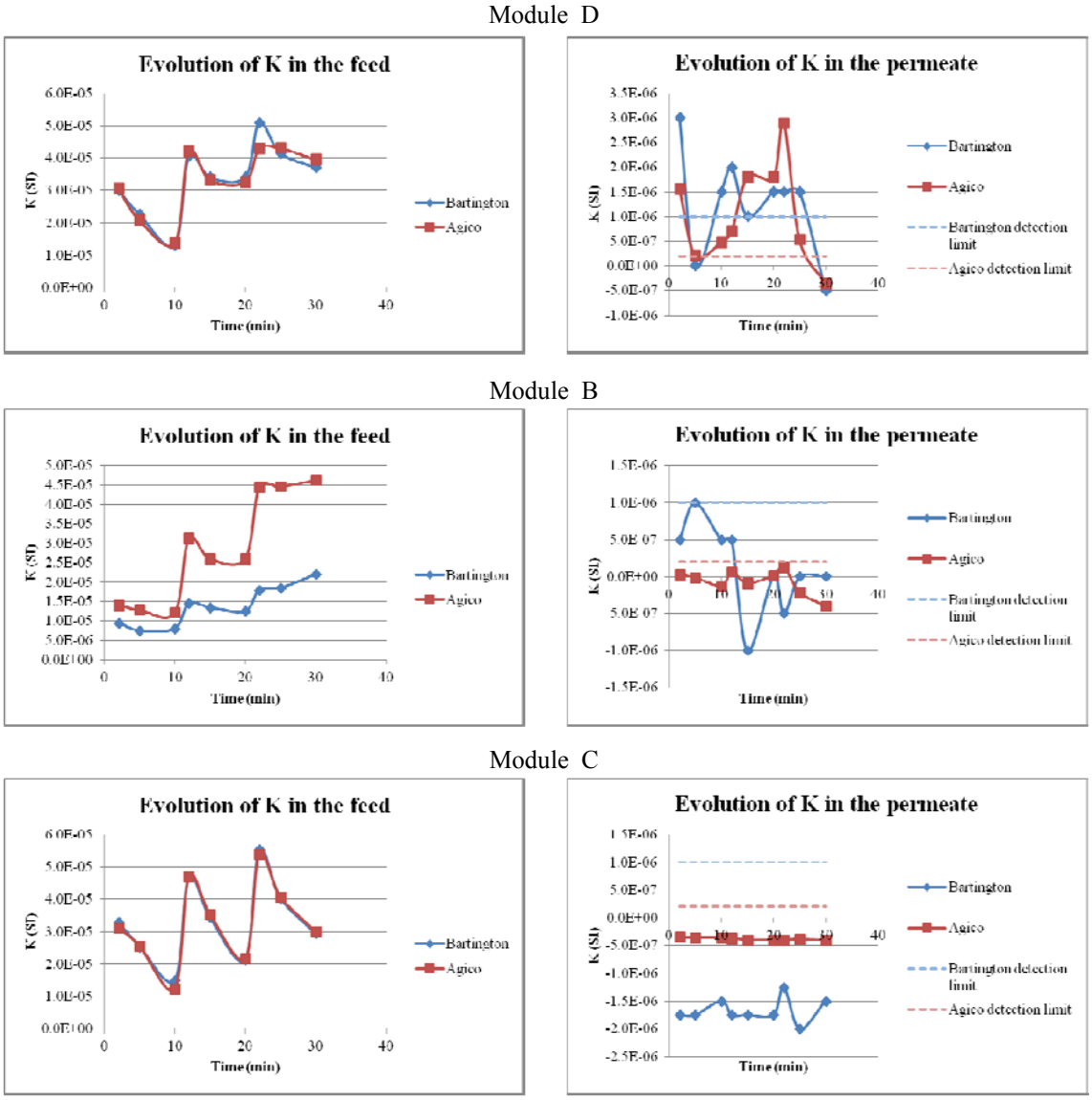

Fig. 6 Variation of the magnetic susceptibility in the feed (left) and in the permeate (right) as a function of time [modules A and D (center of the bundle); B and C (around the bundle)]

Table 6 Parameters for the experiments with the modules (F, H) and (E, G)

Module	Lp0 at 20°C ($L.h^{-1}.m^{-2}.bar^{-1}$)	NP MD (nm) Initial suspension	K (10^6 SI) Initial suspension	NP MD (nm) Feed
E	499	37	4660	35
G	494	46	6742	61
F	505	43	3274	56
H	539	18	4940	36

Module A

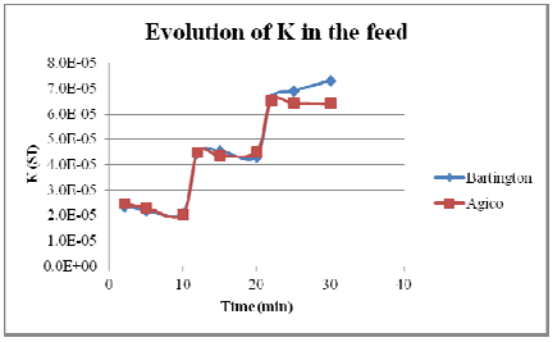

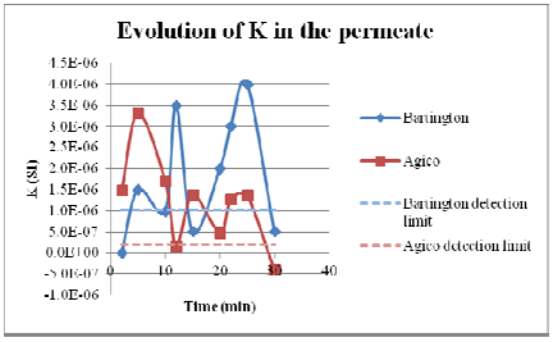

Module D

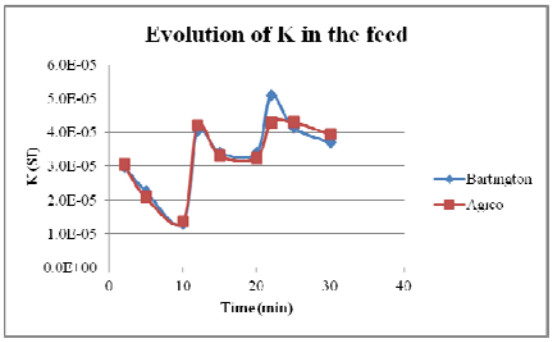

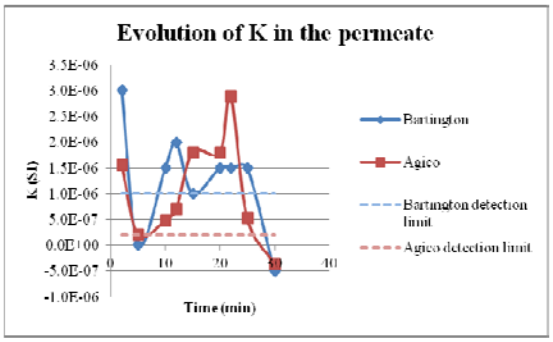

Module B

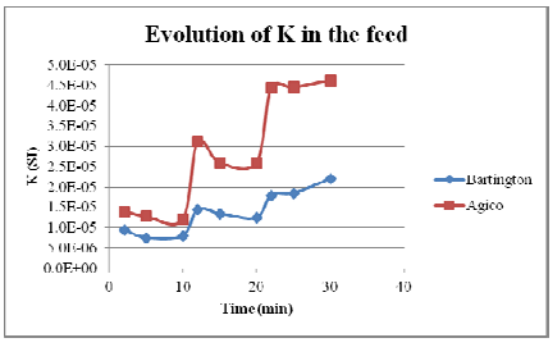

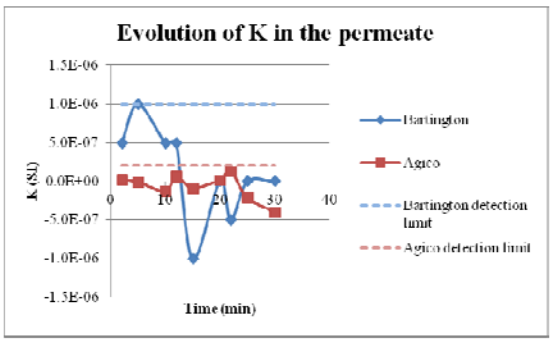

Module C

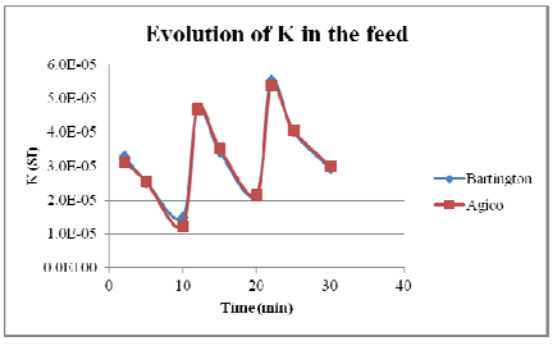

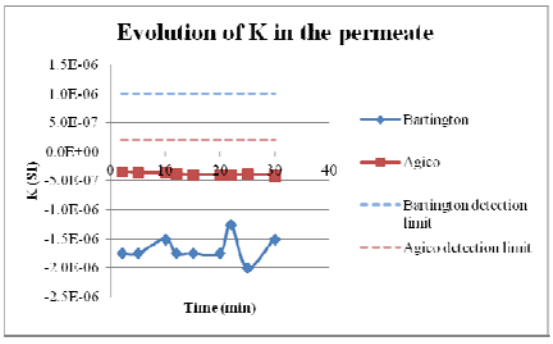

Fig. 7 Variation of the magnetic susceptibility in the feed (left) and in the permeate (right) as a function of time [modules E and G (outside the bundle); F and H (near the module center)]

shows that modules E and G present an advanced ageing with a lack of integrity. This observation is supported by air tests which clearly showed the same defects. This result can be correlated with those in part 3.3.3, for which it was shown that hollow fibers at the centre of the bundle age quicker than hollow fibers placed at the periphery of the bundle. In the case where hollow fibers are collected at the top or bottom of the bundle, these hollow fibers are randomly selected at the center and at the periphery of the bundle. It was shown by numerical simulation that hollow fibers are subjected to different TMPs depending on their position in the bundle (Daurelle *et al.* 2011). Hollow fibers at the periphery of the bundle are subjected to a strong counter pressure and hollow fibers at the center are subjected to the lowest counter pressure. This decrease is concentric from the outside of the bundle towards the center of the bundle. Collecting hollow fibers at the top of the module, in comparison to the bottom, is the place where the thickness of the bundle is the greatest and thus where hollow fibers are less well backwashed. Modules E and G have lost integrity, whereas module F is intact. Therefore, on a bundle and in a logical way, E lost integrity and F maintained integrity. This is not logical on the second bundle with module H showing a loss of integrity and module G being intact. To explain this difference, the issue of sampling at the completion of the modules can be lifted: an industrial module containing 10,000 hollow fibers spread over 12 bundles, each bundle contains 830 hollow fibers. Thus, to achieve the modules (F, H) and (E, G), the whole of a bundle was necessary (400 fibers each). Therefore, a slight sampling error can lead to contradictory results. The backwashing of the module allowed us to easily recover the initial permeability of the membranes.

4. Conclusions

This study has highlighted the heterogeneity of ageing of hollow fibers in an industrial module which had functioned 50 months on site. Among the 18 used modules tested, 5 modules were identified as not being intact. This clearly shows that the ageing of hollow fibers is not homogeneous in an industrial module. It has been clearly established that the location of the fibers towards the module as a whole has little impact. Thus, considering 1 bundle every 3 bundles (modules 1, 2, 3 and 4), 3 modules are intact (2, 3 and 4) for 1 compromised (1). However, this loss of integrity is not detected by conventional investigation air method alone, a methodology with magnetic nanoparticles coupled to an apparatus of high accuracy detection allowed us to highlight this loss of integrity. This latter compared to the other 3 bundles could be explained by the fact that the module was placed horizontally and therefore the pressure was different depending on gravity ; this is only a hypothesis. It therefore appears that the position of the bundle within the module has little influence on the integrity of the hollow fibers. The study of the influence of the fiber's part considered (1st third (5, 8), 2nd third (6, 9) and 3rd third (7, 10)) showed no particular trend, the fibers are ageing identically. The most glaring heterogeneity was observed by studying separately the central and the peripheral fibers of the same bundle. Twice, the module consisting of hollow fibers taken from the center of the bundle showed a loss of integrity unlike the modules consisting of hollow fibers taken from the periphery. This can be explained by a lower backwash pressure at the center of the bundle as shown by numerical simulation. Identically on a bundle, the module made of hollow fibers taken from the zone of lesser thickness (F) is intact whereas the one made from hollow fibers taken from the thicker area (E) is compromised. Finally, this study showed that the integrity test developed by Guo et al. (2010b) could be diverted from its original aim to study the ageing of membranes. The air test allowed us to validate certain results,

especially when the size of the nanoparticles was very close to the size of the pores of the membrane. But the use of nanoparticles, provided a higher defect detection sensibility. A comprehensive study on the hydrodynamics in an industrial module by numerical simulation coupled with an experimental validation will be the subject of a future paper.

References

Choi, S., Yang, J. Suh, C. and Cho, J. (2011), "Use of fluorescent silica particles for checking the integrity of microfiltration membranes", *J. Membrane Sci.*, **367**(1-2), 306-313.

DiLeo, A. and Phillips, M. (1995), "Process for evaluating solute retention characteristics of membranes", US Pate As for the previously used modules, the same observations and the same conclusions can be made regarding the evolution of the magnetic susceptibility in the feed (presence of PAC).
nt 5,**457**,986.

Daurelle, J.V., Q. Derekx, Y. Wyart, K. Glucina and P. Moulin (2011), Use of advanced CFD tool to characterize hydrodynamic of commercial UF membrane module, 8th IWA Leading Edge Amsterdam, Netherland, 8-10 Juin

Fauconnier, N., Pons, J.N. Roger, J. and Bee, A. (1997), "Thiolation of maghemite nanoparticles by dimercaptosuccinic acid", *J. Colloid Inter. Sci*., **194**(2), 427-433.

Giglia, S. and Krishnan, M. (2008), "High sensitivity binary gas integrity test for membrane filters", *J. of Membrane Sci*., **323**(1), 60-66.

Guo, H., Wyart, Y. Perot, J. Nauleau, F. and Moulin, P. (2010), "Application of magnetic nanoparticles for ultrafiltration membrane integrity monitoring at low-pressure operation", *J. of Membrane Sci*., **350**(1-2), 172-179.

Guo, H., Wyart, Y. Perot, J. Nauleau, F. and Moulin, P. (2010), "Low-pressure membrane integrity tests for drinking water treatment: A review", *Water Res*., **44**(1), 41-57.

La, J.M., Glucina, K. Chamant, M. and Simonie, P. (1998), "Acoustic sensor: a novel technique for low pressure membrane integrity monitoring", *Desalination*, **119**(1-3), 73-77.

Moulin, P. (2008) Patent Number(s): FR2901607-A1; EP1862791-A2.

Suh, C., Choi, B. Lee, S. Kim, D. and Cho, J. (2011), "Application of genetic programming to develop the model for estimating membrane damage in the membrane integrity test using fluorescent nanoparticle", *Desalination*, **281**(17), 80-87.

Phattaranawik, J., Fane, A.G. and Wong, F.S. (2008), "Novel membrane-based sensor for online membrane integrity monitoring", *J. Membrane Sci.*, **323**(1), 113-124.

Walsh, M.E., Chaulk, M.P. and Gagnon, G.A. (2005), "Indirect integrity testing on a pilot-scale ultrafiltration membrane", *J. Water Supply: Research and Technology*., AQUA 54, 105-114.

DN

List of symbols

Lp Membrane permeability ($L.h^{-1}.m^{-2}.bar^{-1}$)
MD Mean Diameter (nm)
K Magnetic susceptibility (10^6 SI)
NP Nanoparticles